Blood flow through an axisymmetric stenosis

G Pontrelli
Istituto per le Applicazioni del Calcolo–CNR, Viale del Policlinico, 137, 00161 Roma, Italy

Abstract: This paper studies a steady axisymmetric flow in a constricted rigid tube. A shear-thinning fluid modelling the deformation-dependent viscosity of the blood is proposed. The motion equation is written in vorticity–streamfunction formulation and is solved numerically by a finite difference scheme. The flow pattern with the distributions of pressure and shear stress at the wall are computed. The dependence of the flow on the dimensionless parameters has been investigated and differences from the Newtonian case are discussed.

Keywords: haemodynamics, non-Newtonian models, stenosis, finite difference methods

NOTATION

$\boldsymbol{A}_1$	rate of deformation tensor
$\mathbf{I}$	identity matrix
K	Keulegan–Carpenter number
p	pressure
Q	flowrate
R	radius of the tube
R_0	radius of the undeformed tube
T	period of the imposed flow
$\boldsymbol{T}$	Cauchy tensor stress
U_0	averaged velocity over the section of radius R_0
$\boldsymbol{v}$	velocity vector $= (u, w)$
(x, r, θ)	cylindrical coordinates system
α	Womersley number
$\dot{\gamma}$	shear rate
δ, σ	geometrical parameters
η_0, η_∞	asymptotic apparent viscosities
λ	viscosity ratio
Λ	material parameter
μ	viscosity of the fluid
ρ	density of the fluid
χ	non-dimensional viscosity
ψ	streamfunction
ω	vorticity $= \nabla \times \boldsymbol{v}$

1 INTRODUCTION

The partial occlusion of arteries due to stenotic obstruction is one of the most frequent anomalies in blood circulation. It is well known that, once such obstruction is formed, the blood flow is significantly altered and fluid dynamic factors play an important role as the stenosis continues to develop. Nevertheless, the specific role of these factors is not yet well understood. In recent years, interest in haemodynamic studies has grown since it seems that many cardiovascular diseases are related to the flow conditions in blood vessels [**1**, **2**].

Stenoses have a complex influence on the haemodynamics through and beyond the narrowed arterial segment. Atherosclerotic disease tends to be localized in regions of geometric irregularity such as vessel branch, curved and tapered arteries, and stenotic sites. In the latter case, the flow is disturbed and separation of streamlines, with the formation of eddies, is likely to occur. The fluid mechanical and biochemical effects associated with stenoses have been reported in many studies [**3**–**5**].

Whereas on the one hand the flow disturbances associated with a medium degree of stenosis can be detected through the use of non-invasive means such as the Doppler ultrasound technique, on the other hand a method to detect minor arterial stenosis has not been found. The ability to describe the flow through stenosed vessels would provide the possibility of diagnosing the disease in its earlier stages, even before the stenosis became clinically relevant, and is the basis for surgical intervention. Unfortunately existing measurements and experimental results of blood flows are either incomplete or are not representative of the actual arterial flow. Computational fluid dynamics has revealed a useful, non-invasive tool to evaluate the behaviour of the blood flowing in natural arteries, in surgically reconstructed vessels or through artificial devices. Sometimes, it provides much more information than that available from experiments.

Several studies of fluid dynamics through stenoses have been carried out to evaluate the flow pattern and

The MS was received on 29 February 2000 and was accepted after revision for publication on 21 June 2000.

the shear stresses at the walls under steady and pulsatile flow conditions. Some attempts to study experimentally steady and unsteady flows across a stenosis can be found in references [**6**–**8**]. Other numerical studies deal with blood as a Newtonian fluid [**9**, **10**].

In contrast, it has been observed from experiments that blood behaves as a non-Newtonian fluid at low shear rates and in vessels of small diameter [**5**, **11**, **12**], and exhibits marked shear thinning and significant viscoelastic properties in pulsatile flows [**13**, **14**]. Since the shear rate is low on the downstream side of a stenosis, a correct analysis of the flow pattern should include the shear-thinning characteristics of the blood. More recent results on the flow in stenosed vessels with non-Newtonian models are available in references [**15**–**18**].

An important factor to be investigated in haemodynamics is the wall shear stress, a quantity not easily measurable *in vivo* because of the difficulties arising with the moving wall. Many authors suggested that high shear stress is a factor in the development of atherosclerotic lesions and endothelial damage [**19**]. On the other hand, the low shear stresses downstream from a stenosis are believed to be responsible for adhesion and the deposition of lipids. The constitutive non-linearity of the fluid gives rise to a different mechanism of vorticity diffusion by the contribution of extra terms in the equations with respect to the Newtonian case; both these aspects deserve a more complete understanding.

Some research work on pulsatile flows in complex geometries has been carried out in the last decade [**20**–**22**]. The oscillatory flow over an axisymmetric expansion has been investigated in reference [**23**], where the mechanism of generation and propagation of the vorticity and the dynamics of the boundary layer separation have been studied in detail.

Yeleswarapu [**24**] presents and discusses a generalized Newtonian model used mainly for blood. The model includes a shear-rate-dependent viscosity and has been proved effective for describing blood flows in the typical range of shear rates. The model is first presented in reference [**25**], where a range of values of the material constants is determined. Starting from those issues, the pulsatile and the impulsive flows in straight small vessels has been studied for this model [**26**, **27**].

The present work is a numerical two-dimensional study of the axisymmetric blood flow over a stenosis of a medium degree of contraction; because of the complexity of the constitutive equation, only a steady state case is considered in this paper. A constant flowrate is imposed and the wall deformability is disregarded. The flow dependence on the rheological parameters as well as on the geometry of the stenosis is investigated carefully. Good agreement is obtained with the numerical solution for steady flow in a long and straight pipe and with other results in the Newtonian case.

2 A MATHEMATICAL MODEL FOR BLOOD

While the Newtonian approximation for blood is acceptable in modelling flow in large arteries and in the propagation of a pressure pulse, a non-linear constitutive equation has to be used to describe flow in small vessels or at low shear rates (less than $100\,\mathrm{s}^{-1}$). Since the average shear rate at the wall of arteries is larger than this value, it is generally assumed that blood is a Newtonian fluid in that region. Nevertheless, near the centre of the vessel, or in separated regions of recirculating flow such as the downstream side of a stenosis, the average shear rate value will be small. Non-Newtonian models take into account the effect of a shear-rate-dependent viscosity in some ranges and reduce to a Navier–Stokes fluid in some other ranges.

While the plasma is a fluid with no significant departure from Newtonian behaviour, when red cells are considered, the viscosity of the whole mixture increases noticeably. Marked non-Newtonian properties are evidenced for concentrations greater than 10 per cent [**11**]. It has been shown experimentally that the blood apparent viscosity decreases as shear rate increases. In past years, many constitutive equations have been proposed for the blood to model this shear-thinning property [**12**–**14**]. Some of the equations depend on a large number of parameters, while some others are not completely satisfactory in all deformation ranges and for all flows. Most of such models are based on the following stress–strain rate relationship:

$$\boldsymbol{T} = -p\boldsymbol{I} + \mu(\dot{\gamma})\boldsymbol{A}_1 \tag{1}$$

where

$$\boldsymbol{A}_1 = \operatorname{grad} \boldsymbol{v} + (\operatorname{grad} \boldsymbol{v})^{\mathrm{T}}$$

is the rate of deformation tensor and

$$\dot{\gamma} = [\tfrac{1}{2}\operatorname{tr}(\boldsymbol{A}_1^2)]^{1/2}$$

is the magnitude (i.e. the shear rate).

In references [**24**] and [**25**], the following expression for the blood viscosity function $\mu(\dot{\gamma})$ is suggested:

$$\mu(\dot{\gamma}) = \eta_\infty + (\eta_0 - \eta_\infty)\left[\frac{1 + \log_{\mathrm{e}}(1 + \Lambda\dot{\gamma})}{1 + \Lambda\dot{\gamma}}\right] \tag{2}$$

where η_0 and η_∞ ($\eta_0 \geqslant \eta_\infty$) are the asymptotic apparent viscosities as $\dot{\gamma} \to 0$ and ∞ respectively, and $\Lambda \geqslant 0$ is a material constant with the dimension of time representing the degree of shear thinning [for $\eta_0 = \eta_\infty$, $\mu(\dot{\gamma})$ is a constant and the model reduces to the Newtonian one].

The complex nature of blood is approximated here with a three-parameter shear-thinning model, where the apparent viscosity, μ, is expressed as a decreasing function of the shear rate, $\dot{\gamma}$. Note that, at low shear rates, the apparent viscosity increases considerably. The asymptotic values η_0 and η_∞ are common in many other inelastic shear-thinning models and they are calibrated

by best fitting experimental data, while the value of Λ is found by non-linear regression analysis of viscometric data [**24**, **25**] (see Fig. 1).

3 THE EQUATIONS OF MOTION

Blood is assumed to be an isotropic, homogeneous and incompressible continuum, having constant density, ρ, and the vessel walls are considered rigid and impermeable. Its viscosity is given by equation (2).

The equation of motion is

$$\rho\left(\frac{\partial \boldsymbol{v}}{\partial t} + \boldsymbol{v}\cdot\nabla\boldsymbol{v}\right) = \operatorname{div}\boldsymbol{T} \tag{3}$$

where $\boldsymbol{v}$ is the velocity vector and the body forces are presumed to be negligible.

Consider a cylindrical coordinate system (x, r, θ) having the x axis coincident with the pipe axis. Since an axisymmetric two-dimensional solution is sought, all variables are assumed to be independent of θ and the azimuthal component of $\boldsymbol{v}$ vanishes. The pipe has a circular cross-section whose radius is R_0 everywhere except in a small region centered at $x = 0$ with a mild smooth axisymmetric contraction (stenosis), as described by the following function:

$$\frac{R(x)}{R_0} = 1 - \delta\, \mathrm{e}^{-\sigma x^2} \tag{4}$$

where $R(x)$ is the radius of the tube, $0 \leqslant \delta < 1$ is a measure of the degree of contraction, σ, of its length. The value of σ should be taken to be quite small to guarantee a slowly varying boundary profile. As an example, the cylindrical pipe case is recovered for $\delta = 0$.

The vector equation (3) can be written in scalar form as

$$\begin{aligned}\rho\left(\frac{\partial u}{\partial t} + u\frac{\partial u}{\partial r} + w\frac{\partial u}{\partial x}\right) &= -\frac{\partial p}{\partial r} + \mu(\dot\gamma)\left(\frac{\partial^2 u}{\partial r^2} + \frac{1}{r}\frac{\partial u}{\partial r} + \frac{\partial^2 u}{\partial x^2} - \frac{u}{r^2}\right)\\ &\quad + 2\frac{\partial \mu}{\partial r}\frac{\partial u}{\partial r} + \frac{\partial \mu}{\partial x}\left(\frac{\partial u}{\partial x} + \frac{\partial w}{\partial r}\right)\end{aligned} \tag{5}$$

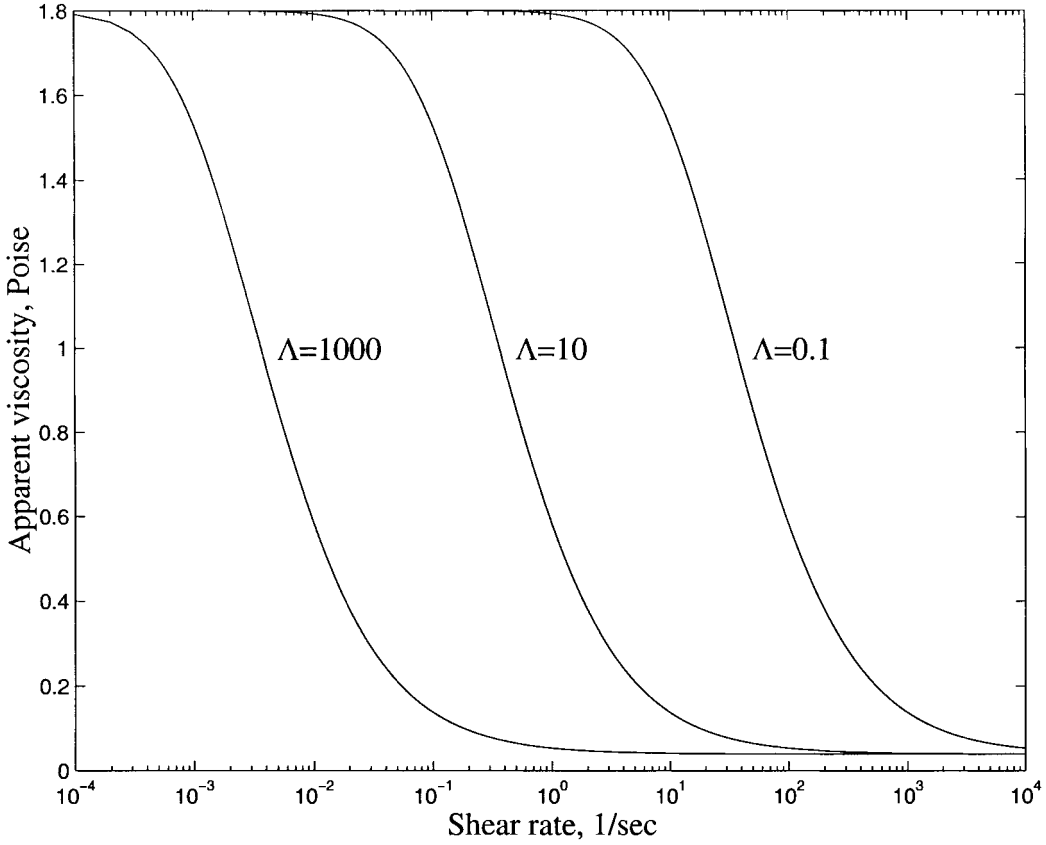

Fig. 1 The shear-rate-dependent viscosity function [equation (2)] for fixed η_0 and η_∞ and three values of Λ (in seconds)

$$\rho\left(\frac{\partial w}{\partial t}+u\frac{\partial w}{\partial r}+w\frac{\partial w}{\partial x}\right)$$
$$=-\frac{\partial p}{\partial x}+\mu(\dot\gamma)\left(\frac{\partial^2 w}{\partial r^2}+\frac{1}{r}\frac{\partial w}{\partial r}+\frac{\partial^2 w}{\partial x^2}\right)$$
$$+\frac{\partial \mu}{\partial r}\left(\frac{\partial u}{\partial x}+\frac{\partial w}{\partial r}\right)+2\frac{\partial \mu}{\partial x}\frac{\partial w}{\partial x} \tag{6}$$

where (u, w) are the components of $\boldsymbol{v}$ in the r and x directions respectively.

A set of non-dimensional variables is now introduced:

$$x\to\frac{x}{R_0},\qquad r\to\frac{r}{R_0},\qquad t\to\frac{tU_0}{R_0}$$
$$u\to\frac{u}{U_0},\qquad w\to\frac{w}{U_0},\qquad p\to\frac{p}{\rho U_0^2}$$
$$\Lambda\to\frac{\Lambda U_0}{R_0},\qquad \lambda=\frac{\eta_0}{\eta_\infty}$$

where U_0 is the velocity averaged over the section of radius R_0. Moreover, two characteristic non-dimensional numbers

$$\alpha=R_0\sqrt{\frac{\rho}{\eta_\infty T}}\qquad\text{and}\qquad K=\frac{U_0 T}{R_0} \tag{7}$$

are introduced in unsteady flows and are defined as the Womersley and the Keulegan–Carpenter numbers respectively (typically, the characteristic time, T, is the period of an imposed flowrate)*.

Following reference [**23**], by cross-differentiating and by subtracting the non-dimensional counterparts of equations (5) and (6), the vorticity–streamfunction formulation is obtained (with ω the azimuthal vorticity and ψ the Stokes streamfunction†) as follows:

$$\frac{\partial\omega}{\partial t}+\frac{1}{r}\frac{\partial\psi}{\partial r}\frac{\partial\omega}{\partial x}-\frac{1}{r}\frac{\partial\psi}{\partial x}\frac{\partial\omega}{\partial r}+\frac{\omega}{r^2}\frac{\partial\psi}{\partial x}$$
$$=\frac{1}{\alpha^2}\left[\chi\left(\frac{\partial^2\omega}{\partial x^2}+\frac{\partial^2\omega}{\partial r^2}+\frac{1}{r}\frac{\partial\omega}{\partial r}-\frac{\omega}{r^2}\right)+2\frac{\partial\chi}{\partial x}\frac{\partial\omega}{\partial x}+\frac{\partial\chi}{\partial r}\right.$$
$$\times\left(2\frac{\partial\omega}{\partial r}+\frac{\omega}{r}\right)+2\frac{\partial^2\chi}{\partial r\,\partial x}\left(\frac{1}{r^2}\frac{\partial\psi}{\partial x}-\frac{2}{r}\frac{\partial^2\psi}{\partial r\,\partial x}\right)$$
$$\left.+\left(\frac{\partial^2\chi}{\partial x^2}-\frac{\partial^2\chi}{\partial r^2}\right)\left(\frac{1}{r}\frac{\partial^2\psi}{\partial r^2}-\frac{1}{r}\frac{\partial^2\psi}{\partial x^2}-\frac{1}{r^2}\frac{\partial\psi}{\partial r}\right)\right] \tag{8}$$

* In the steady case, T is the unit time R_0/U_0 and $\alpha^2=\rho R_0 U_0/\eta_\infty$ is the Reynolds number.

† The following relations between velocity components, vorticity and streamfunction hold:

$$\omega=\frac{\partial u}{\partial x}-\frac{\partial w}{\partial r},\qquad u=-\frac{1}{r}\frac{\partial\psi}{\partial x},\qquad w=\frac{1}{r}\frac{\partial\psi}{\partial r}$$

where

$$\chi(\dot\gamma)=1+(\lambda-1)\frac{1+\log_e(1+\Lambda\dot\gamma)}{1+\Lambda\dot\gamma}$$

and

$$\dot\gamma^2=\frac{4}{r^2}\left[\frac{1}{r^2}\left(\frac{\partial\psi}{\partial x}\right)^2+\left(\frac{\partial^2\psi}{\partial r\,\partial x}\right)^2-\frac{1}{r}\frac{\partial\psi}{\partial x}\frac{\partial^2\psi}{\partial r\,\partial x}\right]$$
$$+\frac{1}{r^2}\left(\frac{\partial^2\psi}{\partial r^2}-\frac{1}{r}\frac{\partial\psi}{\partial r}-\frac{\partial^2\psi}{\partial x^2}\right)^2$$

are the dimensionless generalized viscosity and the squared shear rate respectively.

It is worth noting that the right-hand side of equation (8) is made up of many terms of different physical significance due to the variable viscosity and expresses a transport and diffusion of vorticity from the boundary to the main stream. The combined non-linear effect of these components alters the dynamics of the vorticity and is important for understanding the formation, the development and the separation of the boundary layer. Note that in a fluid with constant viscosity, all the terms within the square brackets, except the first one, disappear.

Vorticity and streamfunction are related by the Poisson equation

$$-\omega r=\frac{\partial^2\psi}{\partial x^2}+\frac{\partial^2\psi}{\partial r^2}-\frac{1}{r}\frac{\partial\psi}{\partial r} \tag{9}$$

The velocity field, automatically satisfying the continuity equation, can be computed from the streamfunction (see reference [**28**]). The boundary conditions at the wall can be expressed easily by choosing a system of coordinates where the wall coincides with a constant coordinate curve. Therefore, a shearing coordinate transformation is applied (see reference [**29**]), replacing the r coordinate with a new z coordinate defined by

$$z(x, r)=\frac{r}{R(x)}$$

The Poisson equation (9) and the motion equation (8) can be expressed in terms of the new coordinates (x, z) respectively, as follows:

$$-\omega r=\frac{\partial^2\psi}{\partial x^2}+\left[\left(\frac{\partial z}{\partial x}\right)^2+\left(\frac{\partial z}{\partial r}\right)^2\right]\frac{\partial^2\psi}{\partial z^2}$$
$$+2\frac{\partial z}{\partial x}\frac{\partial^2\psi}{\partial x\,\partial z}+\left(\frac{\partial^2 z}{\partial x^2}-\frac{1}{r}\frac{\partial z}{\partial r}\right)\frac{\partial\psi}{\partial z} \tag{10}$$

and

$$\frac{\partial\omega}{\partial t}=-\mathscr{J}(\omega,\psi)-\mathscr{K}(\omega,\psi)+\mathscr{D}(\omega,\psi) \tag{11}$$

where the operators $\mathscr{J}$, $\mathscr{K}$ and $\mathscr{D}$ represent the Jacobian term, the additional non-linear term given by the axisymmetry and the diffusive terms in the new coordinate

system (x, z) respectively. The boundary conditions associated with the physical problem are

$$\begin{aligned} &\psi = KQ && \text{at } z = 1 \\ &\omega = -\frac{1}{R^3}\left[1 + \left(\frac{\mathrm{d}R}{\mathrm{d}x}\right)^2\right]\frac{\partial^2\psi}{\partial x^2} = 0 && \text{at } z = 1 \\ &\omega = \psi = 0 && \text{at } z = 0 \end{aligned} \tag{12}$$

where $Q > 0$ is a constant non-dimensional assigned flowrate. At each time and at considerable distance upstream and downstream from the stenosis (formally at $x \to \pm\infty$), a uniform flow consistent with equation (12) is imposed.

Though a steady case is considered here, the solution is obtained as the limit of the evolution problem [equation (11)]. An initial condition consistent with the above boundary conditions has to be chosen; as a reference case, the Hagen–Poiseuille flow at $t = 0$ was chosen. Its effect disappears after a short transient when the steady solution is developed.

4 NUMERICAL METHOD

Although finite elements and finite volume methods are well suited to solving haemodynamical problems, in the infinite strip transformed domain a finite difference method is easily and cheaply employed. As physical intuition suggests, a better resolution is required near the walls $(z \to 1)$ and downstream from the contraction region $(0 < x < \sigma)$. As a consequence, a stretching of the z axis by a new coordinate ξ was introduced; ξ is defined by

$$z = \frac{\tanh(a\xi)}{\tanh(a)} \tag{13}$$

where a is a stretching parameter. Similarly, a stretching of the x axis by a new coordinate η is introduced; η is defined by

$$x = b\tanh^{-1}(\eta) + x_0 \tag{14}$$

where b and x_0 are stretching and shifting parameters respectively (see Fig. 2).

In the new system of coordinates (η, ξ), equations (10) and (11) are discretized by using second-order finite difference schemes over a uniformly spaced grid on the $(-1, 1) \times [0, 1]$ domain. Near to the boundaries, first-order approximations are used, and the truncation error is controlled by the grid refinement. The non-linear Jacobian term $\mathcal{J}(\omega, \psi)$ of the equation of motion is treated using the Arakawa scheme which reduces aliasing errors and guarantees the conservation of some physical quantities [**30**]. The motion equation (11) is integrated in time using the low-storage third-order Runge–Kutta scheme [**31**], the time step chosen is small enough that the stability conditions on the convective and diffusive terms are preserved [**32**]. Note that the non-Newtonian case studied here has a more severe diffusive stability condition than the Newtonian case.

The discretization of the Poisson equation leads, three times per time step, to a $(N_x \times N_r)^2$ linear system, where N_x and N_r are the number of grid points in the x and r directions respectively. The solution of this nine-diagonal, diagonally dominant, non-symmetric linear system is obtained by the biconjugate gradient-stabilized method [**33**], preconditioned by an incomplete LU factorization [**34**]. The method, though still expensive, is computationally efficient and accurate.

5 COMPUTATIONAL RESULTS

The many parameters that the problem is depending on have been ranged around some typical values to obtain results of biomechanical interest. They are chosen as equal for the Newtonian (N) and non-Newtonian (NN) flows to allow a comparison of the two cases. The following physical parameters are assigned [see definitions (7)]:

$$K = 1, \qquad Q = 50, \qquad \alpha^2 = 10$$

In the steady flow case studied here, the Reynolds number $Re = K\alpha^2$ is within the physiological range of blood flow in small vessels [**5**, **11**]. The geometrical parameters concerning the stenosis profile in equation (4) are

$$\sigma = 0.8, \qquad \delta = 0.3$$

corresponding to a degree of contraction of about 50 per cent.

For the set of parameters considered, the number of grid points along the stretched axes η and ξ are $N_x = 256$ and $N_r = 64$ respectively. This large number of points is necessary in the NN case because of the higher-order derivatives and the non-linearities,

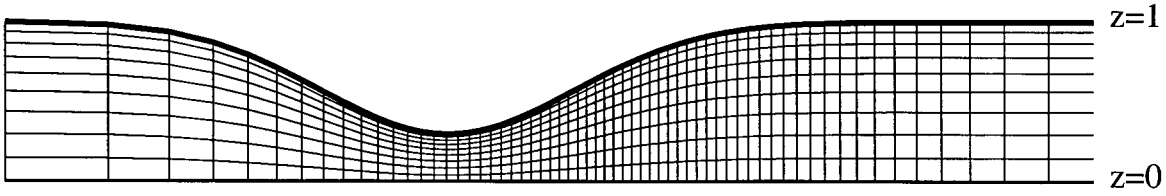

Fig. 2 The computational grid

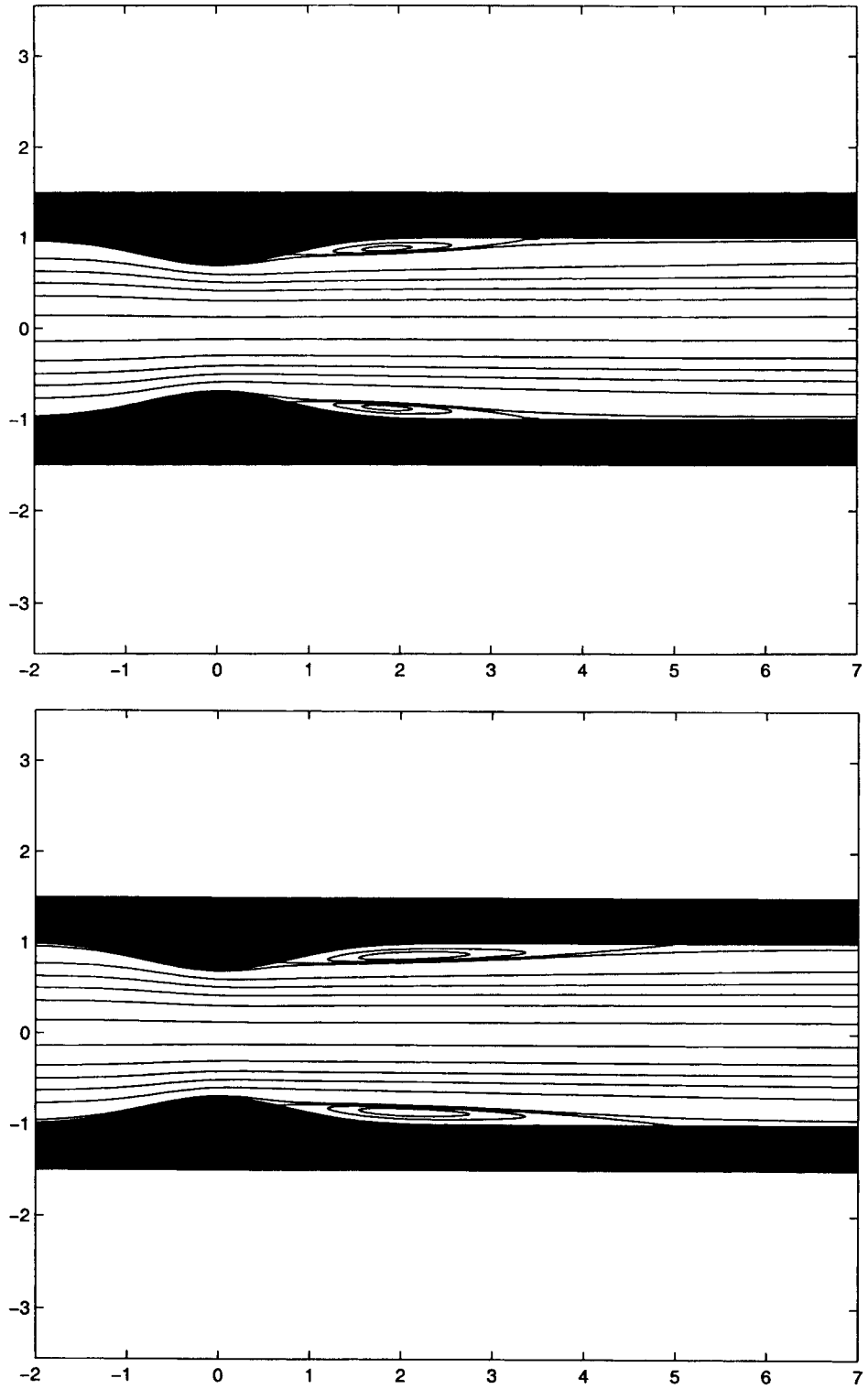

Fig. 3 Streamlines for a 50 per cent stenosis. Comparison between N (top) and NN (bottom) cases

allowing a sufficient resolution near critical regions; the solution turns out to be convergent, since no significant improvement has been found for a finer grid.

The time step has been selected as small at $\Delta t = 10^{-6}$ in order to guarantee the convective and diffusive stability conditions in all cases [**32**]. Note that Δt should be reduced when α^2 is smaller or when K is larger.

The parameters in equations (13) and (14) are fixed as

$$a = 1.2, \qquad b = 8, \qquad x_0 = 3$$

The steady state solution is computed as a limit of the time-dependent case. Simulations run until the convergence of the solution is achieved (i.e. the relative error

between two subsequent values of $\max_{x,z}|\omega(x, z)|$ is less than 10^{-8}). In NN simulations 50 000–70 000 time steps are required.

Differences between N and NN flows become significant in most cases and are pointed out below. In the examples presented here, the rheological parameters in the NN case have the following values:

$$\lambda = 40, \qquad \Lambda = 50$$

Other numerical experiments, made with other parameters, give the same qualitative results and provide similar conclusions.

5.1 Streamlines

For the values of the parameters considered, the separation of the streamlines from the wall can be observed, with the formation of a recirculation zone between the forward flowing main stream and the boundary. The separation and the reattachment points are clearly visible, the latter is moved downstream with Λ (Fig. 3).

5.2 Flow velocities

The velocity profiles are of some interest since they provide a detailed description of the flow field. The region of reversal flow is evidenced in Fig. 4. In this region, the components of velocity undergo a change in sign, and their magnitude is slightly larger in the NN case. Conversely, in the main stream the velocity is greater in the Newtonian case.

5.3 Pressure losses and wall shear stress

In the presence of a narrowing, the flow exhibits a resistance and hence an increase in the shear stress (i.e. the wall vorticity) and a pressure drop. These are quantities of physiological relevance. A zero pressure at the inlet is assigned, since it is determined up to some constant. A rapid fall in pressure is observed as the occlusion is approached, and the local minimum is attained in correspondence with the separation point (Fig. 5).

Since there is no reliable method of determining wall shear stress experimentally near the regions of reversal flow, the numerical experiments offer a sufficient approximation of the fields. The shear stress increases sharply before the contraction and has a peak value near the centre of the throat; downstream it decreases and reverses direction. The large zone of recirculation is evidenced by the negative values of the shear stress (Fig. 5). The values of the extrema are larger in the N case. As for the streamlines, the vorticity contours are moved further downstream in the NN case.

Because of the rigid wall assumption, the present investigation has to be interpreted as a model study. The results, however, are indicative of the importance of the blood rheology and they are in qualitative agreement with those of other models existing in the literature [**15**, **17**, **18**], and with experimental results [**6**].

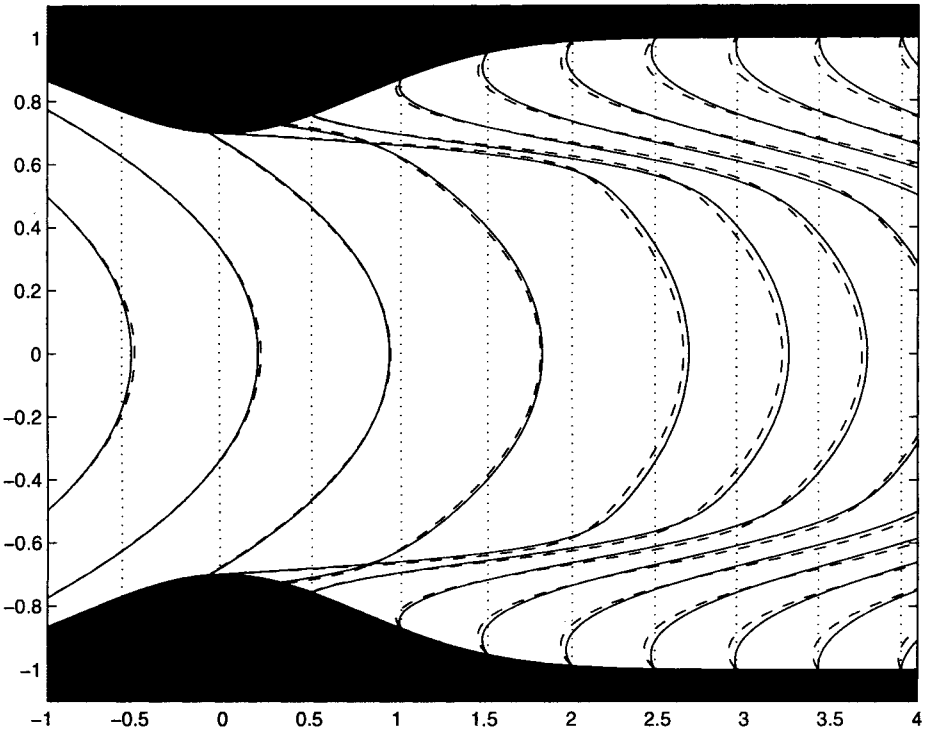

Fig. 4 Velocity profiles downstream from the stenotic region. Comparison between N (continuous line) and NN (dashed line) cases

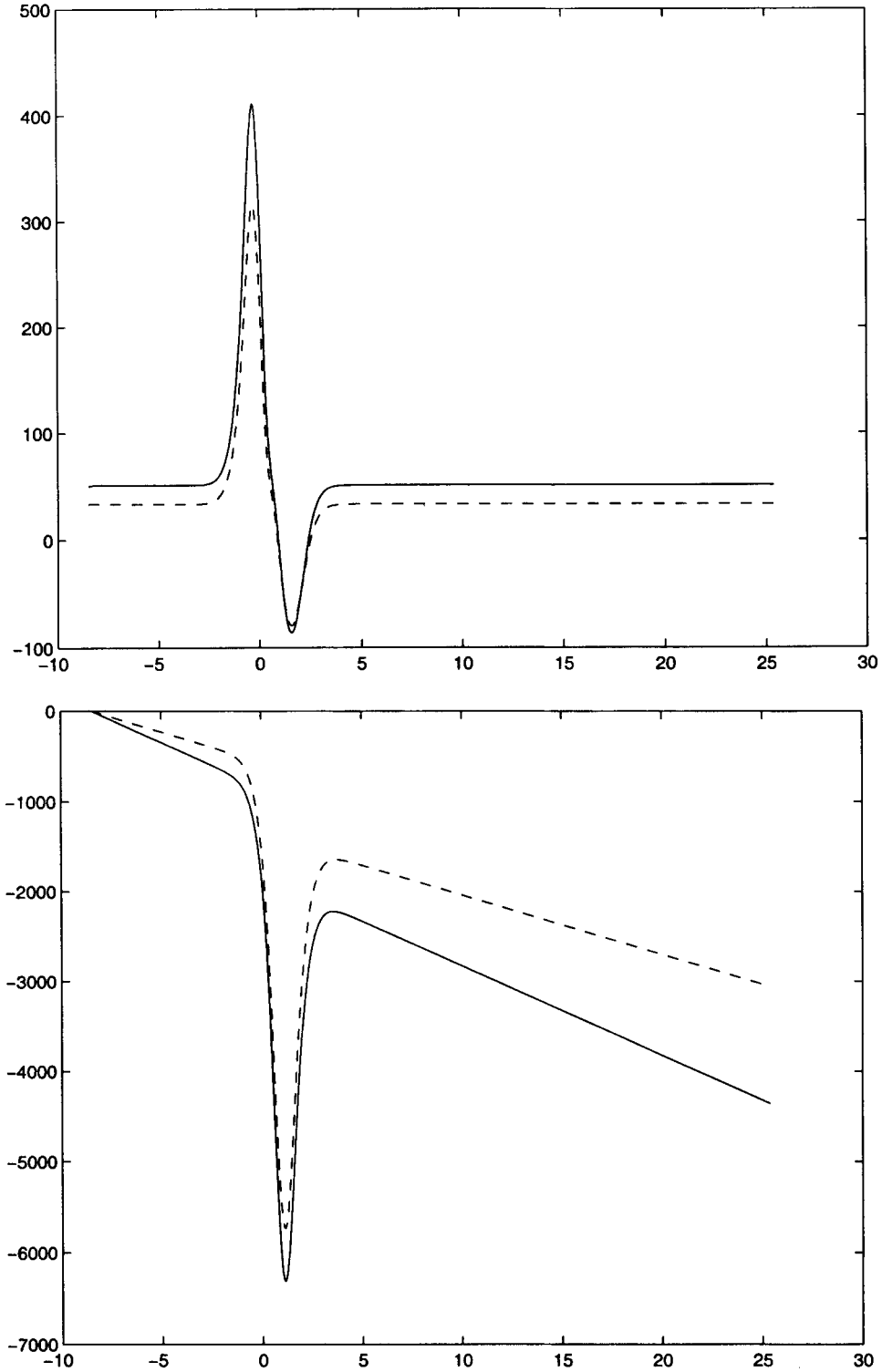

Fig. 5 Shear stress (top) and pressure drop (bottom) at the wall. Comparison between N (continuous) and NN (dashed) cases

6 CONCLUSIONS

Localized narrowing of an artery is a frequent effect or a cause of vascular diseases. Such constriction disturbs normal blood flow through the vessel, and there is considerable evidence that fluid dynamic factors play a significant role in the development and progression of disease itself. Mathematical models and numerical simulations offer an alternative and non-invasive tool for obtaining detailed and realistic descriptions of complex arterial flows.

A simulation of the blood flow through a stenotic arterial segment has been carried out. Though the important effect of unsteadiness is disregarded, this work shows the combined role played by the geometry and the material non-linearity on the flow field.

The results demonstrate that the non-Newtonian character of the blood, in some typical regimes, modifies the flow pattern, even beyond the contracted region and reduces the pressure drop and the shear stress at the wall across the stenosis. Therefore the model presented is able to predict the main characteristics of the physiological flows and be of some interest in biomedical applications. However, an estimate of the characteristic parameters should be addressed on the basis of existing measurements. A time-dependent flow with an oscillatory forcing will be the object of a later work.

ACKNOWLEDGEMENTS

The author wishes to thank Professor K. R. Rajagopal for some stimulating discussions about the model used and is also grateful to Professor G. Pedrizzetti for many valuable comments. This work has been supported by the Progetto Strategico: Metodi e Modelli matematici nello studio di fenomeni biologici of CNR, Italy, 1999.

REFERENCES

1 **Friedman, M. H., Bargeron, C. B., Duncan, D. D., Hutchins, G. M.** and **Mark, F. F.** Effects of arterial compliance and non-Newtonian rheology on correlations between intimal thickness and wall shear. *Trans. ASME, J. Biomech. Engng*, 1992, **114**, 317–320.

2 **Taylor, C., Hughes, T.** and **Zarins, C.** Computational investigations in vascular disease. *Computers in Physics*, 1996, **10**(3), 224–232.

3 **Goldsmith, H. L.** and **Skalak, R.** Hemodynamics. *Ann. Rev. Fluid Mechanics*, 1975, **7**, 213–247.

4 **Pedley, T. J.** *The Fluid Mechanics of Large Blood Vessels*, 1980 (Cambridge University Press, Cambridge).

5 **Ku, D. N.** Blood flow in arteries. *Ann. Rev. Fluid Mechanics*, 1997, **29**, 399–434.

6 **Young, D. F.** and **Tsai, F. Y.** Flow characteristics in models of arterial stenoses—I. Steady flow. *J. Biomechanics*, 1973, **6**, 395–410.

7 **Young, D. F.** and **Tsai, F. Y.** Flow characteristics in models of arterial stenoses–II. Unsteady flow. *J. Biomechanics*, 1973, **6**, 547–559.

8 **Siouffi, M., Pelissier, R., Farahifar, D.** and **Rieu, R.** The effect of unsteadiness on the flow through stenoses and bifurcations. *J. Biomechanics*, 1984, **17**(5), 299–315.

9 **Misra, J. C.** and **Chakravarty, S.** Flow in arteries in the presence of stenosis. *J. Biomechanics*, 1986, **19**(11), 907–918.

10 **Tu, C., Deville, M., Dheur, L.** and **Vanderschuren, L.** Finite element simulation of pulsatile flow through arterial stenosis. *J. Biomechanics*, 1992, **25**(10), 1141–1152.

11 **Chien, S., Usami, S.** and **Skalak, R.** Blood flow in small tubes. In *Handbook of Physiology*, Sec. 2, *The Cardiovascular System*, Vol. 4 (Eds M. Renkins and C. C. Michel), 1984, pp. 217–249 (American Physiology Society, Bethesda, Maryland).

12 **Mann, D. E.** and **Tarbell, J. M.** Flow of non-Newtonian blood analog fluids in rigid curved and straight artery models. *Biorheology*, 1990, **27**, 711–733.

13 **Phillips, W. M.** and **Deutsch, S.** Toward a constitutive equation for blood. *Biorheology*, 1975, **12**, 383–389.

14 **Oiknine, C.** Rheology of the human blood. In *Advances in Cardiovascular Physics* (Ed. T. Kenner), 1983, Vol. 5, Part I, pp. 1–25 (Karger, Basel).

15 **Nakamura, M.** and **Sawada, T.** Numerical study on the flow of a non-Newtonian fluid through an axisymmetric stenosis. *J. Biomech. Engng*, 1988, **110**, 137–143.

16 **Chakravarty, S.** and **Datta, A.** Effects of stenosis on arterial rheology through a mathematical model. *Math. Comput. Modelling*, 1989, **12**(12), 1601–1612.

17 **Misra, J. C., Patra, M. K.** and **Misra, S. C.** A non-Newtonian fluid model for blood flow through arteries under stenotic conditions. *J. Biomechanics*, 1993, **26**, 1129–1141.

18 **Tu, C.** and **Deville, M.** Pulsatile flow of non-Newtonian fluids through arterial stenoses. *J. Biomechanics*, 1996, **29**(7), 899–908.

19 **Zhao, S. Z., Xu, X. Y.** and **Collins, M. W.** The numerical analysis of fluid–solid interactions for blood flow in arterial structures. Part 1: a review of models for arterial wall behaviour. *Proc. Instn Mech. Engrs, Part H, Journal of Engineering in Medicine*, 1998, **212**(H1), 39–59.

20 **Mei, R.** and **Adrian, M. J.** Flow past a sphere with an oscillation in the free-stream velocity and unsteady drag at finite Reynolds number. *J. Fluid Mechanics*, 1992, **233**, 613–631.

21 **Tutty, O. R.** Pulsatile flow in a constricted channel. *J. Biomech. Engng*, 1992, **114**, 50–54.

22 **Tutty, O. R.** and **Pedley, T. J.** Oscillatory flow in a stepped channel. *J. Fluid Mechanics*, 1993, **247**, 179–204.

23 **Pedrizzetti, G.** Unsteady tube flow over an expansion. *J. Fluid Mechanics*, 1996, **310**, 89–111.

24 **Yeleswarapu, K. K.** Evaluation of continuum models for characterizing the constitutive behavior of blood. PhD thesis, Department of Mechanical Engineering, University of Pittsburgh, 1996.

25 **Yeleswarapu, K. K., Antaki, J. F., Kamaneva, M.** and **Rajagopal, K. R.** The flow of blood in the tubes: theory and experiments. *Mech. Res. Commun.*, 1998, **25**, 257–262.

26 **Pontrelli, G.** Pulsatile blood flow in small vessels. In *Simulations in Biomedicine IV* (Eds H. Power, C. A.

Brebbia and J. Kenny), 1997, pp. 145–155 (Computational Mechanics Publications, Southampton).

27 **Pontrelli, G.** Blood flow through a circular pipe with an impulsive pressure gradient. *Math. Models and Meth. in Appl. Sci.*, 2000, **10**(2), 187–202.

28 **Batchelor, G. K.** *An Introduction to Fluid Dynamics*, 1967 (Cambridge University Press, Cambridge).

29 **Eiseman, P. R.** Grid generation for fluid mechanics computation. *Ann. Rev. Fluid Mechanics*, 1985, **17**, 487–522.

30 **Arakawa, A.** Computational design for long term numerical integration of the equation of fluid motion: two dimensional incompressible flow. Part I. *J. Comput. Physics*, 1966, **1**, 119–143.

31 **Williamson, J. H.** Low-storage Runge–Kutta schemes. *J. Comput. Physics*, 1980, **35**, 48–56.

32 **Fletcher, C. A.** *Computational Techniques for Fluid Dynamics I*, 1988 (Springer-Verlag, Berlin).

33 **van der Vorst, H. A.** BiCGSTAB—a fast and smoothly converging variant of Bi-CG for the solution of non-symmetric linear systems. *SIAM J. Sci. Stat. Comput.*, 1992, **13**(2), 631–644.

34 **Meijerink, J. A.** and **Van der Vorst, H. A.** Guidelines for the usage of incomplete decompositions in solving sets of linear equations as they occur in practical problems. *J. Comput. Physics*, 1981, **44**, 134–146.